Optical Properties of Graphene Nanoribbons Encapsulated in Single-Walled Carbon Nanotubes

Alexander I. Chernov,[†,*] Pavel V. Fedotov,[†] Alexandr V. Talyzin,[‡] Inma Suarez Lopez,[†] Ilya V. Anoshkin,[§] Albert G. Nasibulin,[§] Esko I. Kauppinen,[§] and Elena D. Obraztsova[†]

[†]A.M. Prokhorov General Physics Institute, Russian Academy of Sciences, 38 Vavilov Street, 119991, Moscow, Russia, [‡]Department of Physics, Umeå University, S-90187 Umeå, Sweden, and [§]Department of Applied Physics, Aalto University School of Science, P.O. Box 15100, FI-00076, Espoo, Finland

ABSTRACT We report the photoluminescence (PL) from graphene nanoribbons (GNRs) encapsulated in single-walled carbon nanotubes (SWCNTs). New PL spectral features originating from GNRs have been detected in the visible spectral range. PL peaks from GNRs have resonant character, and their positions depend on the ribbon geometrical structure in accordance with the theoretical predictions. GNRs were synthesized using confined polymerization and fusion of coronene molecules. GNR@SWCNTs material demonstrates a bright photoluminescence both in infrared (IR) and visible regions. The photoluminescence excitation mapping in the near-IR spectral range has revealed the geometry-dependent shifts of the SWCNT peaks (up to 11 meV in excitation and emission) after the process of polymerization of coronene molecules inside the nanotubes. This behavior has been attributed to the strain of SWCNTs induced by insertion of the coronene molecules.

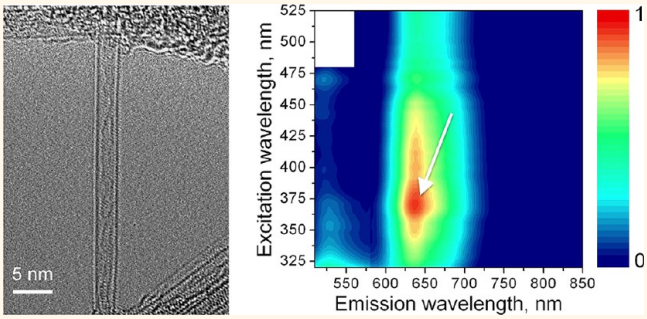

KEYWORDS: single-walled carbon nanotubes · graphene nanoribbons · coronene · photoluminescence · one-dimensional graphene structure

Graphene nanoribbons (GNRs) with a width less than 20 nm are interesting as a 1D material with an optical band gap. The gap can be estimated by photoluminescence (PL) spectroscopy. To the best of our knowledge all previous attempts to measure the PL of GNRs have failed. In this work we have registered the PL of narrow GNRs formed from coronene molecules inside single-walled carbon nanotubes (SWCNTs).

SWCNTs have unique physical properties due to their one-dimensional structure.[1] Optical transitions in SWCNTs are determined by the electron confinement due to the circumference of the carbon nanotube, leading to a density of states comprising a set of van Hove singularities, by the binding energy of an attractive Coulomb interaction between an electron and a hole and by the electron−electron interaction. SWCNT debundling in suspension revealed new ways for characterization of chirality of semiconducting carbon nanotubes: optical absorption and photoluminescence spectroscopies.[2,3] PL has become a very informative and convenient method for studying SWCNTs.[4] This triggered extensive experimental research on the electronic structure and optical properties of SWCNTs. Carbon nanotubes can be successfully employed in biomarker applications,[5] photonics,[6] photovoltaics,[7] and optoelectronics.[8] Many studies were aimed to increase the PL quantum yield of carbon nanotube-based materials in different spectral regions. The reported values of PL quantum yields[9−11] significantly vary depending on the environment, functionalization, and bundling of the nanotubes. The filling of SWCNTs with organometallic molecules enhances a near-infrared PL, as demonstrated recently by Liu *et al.*[12] Filling SWCNTs with molecules opens up a possibility to enhance the PL quantum yield and at the same time to obtain PL emission in different spectral regions, which is very attractive for different types of applications.

* Address correspondence to al.chernov@nsc.gpi.ru.

Received for review May 13, 2013 and accepted June 24, 2013.

Published online June 24, 2013
10.1021/nn4024152

GNRs are another sp^2-hybridized carbon nanomaterial. Electronic properties of GNRs strongly depend on their width and edge shape.[13] For instance, narrowing the width of a GNR increases its band gap.[14,15] Various techniques have been reported for formation of GNRs including chemical synthesis,[16] unzipping of multiwalled carbon nanotubes,[17] and bottom-up fabrication.[18] The size (width and length) of the ribbons and precision of their formation remain important issues in synthesis. The width of the GNRs should be less than 2 nm in order to follow the change of physical properties driven by quantum-sized effects (due to the transition from 2D to 1D material) and to investigate the band gap opening with PL spectroscopy. Different molecules have been recently used as building blocks for "bottom to top" synthesis of hydrogen-terminated nanoribbons[18] using a surface-assisted dehydrogenation and polymerization. Recent experiments have demonstrated the possibility to form narrow GNRs inside the nanotubes using polycyclic aromatic hydrocarbon (PAH) molecules as precursors.[19] Carbon nanotubes also have been used as nanoscale chemical reactors to synthesize sulfur-terminated nanoribbons using various organic molecules.[20] Theoretical studies show that the termination of the edges with different types of molecules significantly influences the electronic structure of the GNR.[21,22] The space inside SWCNTs provides geometrical conditions for formation of one-dimensional structures using chain polymerization of "nanographene" molecules (*e.g.*, coronene and perylene) into nanoribbons.[23] Molecules placed inside SWCNTs are well protected from the external environment and can form inner structures that are thermodynamically unstable in the absence of an encapsulating template. Different configurations of GNRs have been predicted to form inside the nanotubes.[24,25] Confinement determines the behavior of molecules encapsulated in SWCNTs.[26] Therefore, variously shaped nanoribbons can possibly be obtained by selection of specific types of host tubes, PAH precursors, and parameters of polymerization reactions.

In this article we report a photoluminescence excitation (PLE) study of GNRs encapsulated inside SWCNTs. The results provide decisive evidence for successful formation of GNRs and allow a detailed characterization of their width and relation to diameters of encapsulating SWCNTs. It is found that GNR@SWCNTs have bright PL in the visible spectral range. The response is resonant and originates from the encapsulated GNRs. PL peak positions depend on the ribbon structure, in accordance with the theoretically predicted values. Simultaneously, GNR@SWCNTs emit in the IR region. This contribution comes from the host SWCNTs. The change in the host SWCNT optical band gap relative to that of initial nonfilled SWCNTs has been revealed.

RESULTS AND DISCUSSION

High-resolution electron microscopy (HRTEM) image of the sample (Figure 1) demonstrates the produced GNRs inside SWCNTs. Generally, almost all nanotubes are filled with GNRs.

The structure of nanoribbons is not uniform in width and contains helical twists. Such twists unambiguously prove the formation of GNRs rather than other types of structures inside SWCNTs.[19,27] Twisting has also been shown to contribute to the band gap values of the nanoribbon.[28]

We used two types of SWCNTs[29] with different average diameters as a template for the GNR formation in order to form nanoribbons with various widths and,

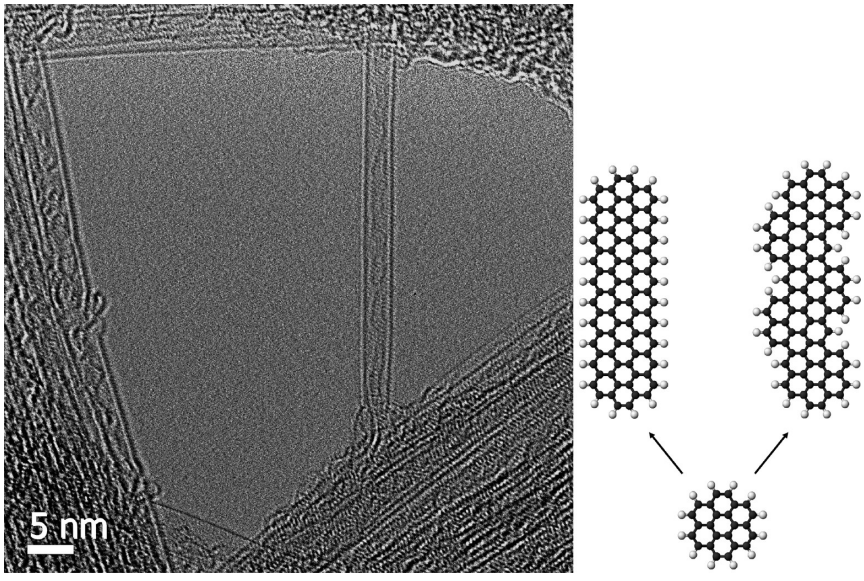

Figure 1. HRTEM image of SWCNTs with GNRs formed inside and a schematic representation of GNR formation from a coronene molecule.

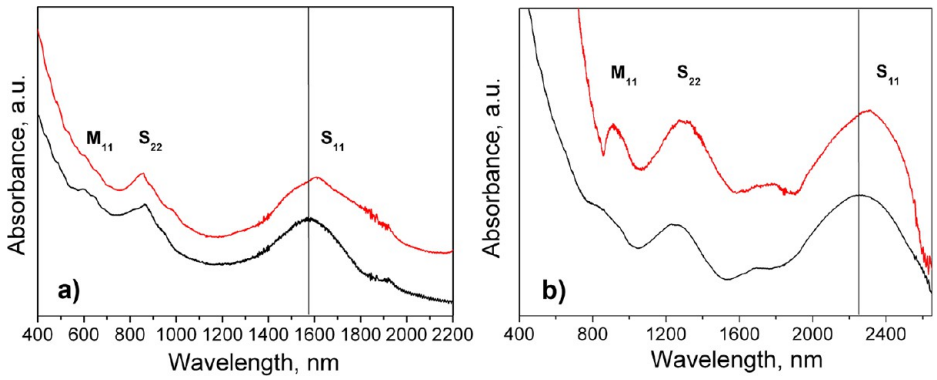

Figure 2. UV−vis−NIR absorption spectra of pristine SWCNTs (in black) and GNR@SWCNTs (in red). (a) SWCNTs with an average diameter of 1.3 nm. (b) SWCNTs with an average diameter of 1.9 nm.

therefore, with different electronic structure. The absorption spectra of these nanotubes before and after the synthesis are shown in Figure 2. The average diameter for narrow tubes is 1.3 nm and for wider ones −1.9 nm.[30] After the synthesis E_{11s} peaks of SWCNTs for both samples became wider and demonstrate a red shift. For the narrow tubes this shift is about 18 meV, and for the wide tubes it is 8 meV.

The peak width increase can be explained by the partial filling of the nanotubes with nanoribbons and by the strain-induced changes of electronic structure in the filled SWCNTs.[31,32] Nanotubes with an average diameter of 1.3 nm are close to the predicted size limit for insertion of coronene molecules;[33] therefore the induced strain in such nanotubes could be higher, resulting in the higher values of the peak shifts compared to those for the larger diameter tubes.

Raman spectroscopy has revealed some typical features appearing after the formation of GNR@SWCNTs. Besides Raman lines assigned to initial carbon nanotubes, new peaks are found in the D and G band regions. The highest intensities of new peaks (1323, 1350, and 1404 cm^{-1}) are observed when a 2.41 eV excitation wavelength is used. Positions of these peaks are close to the reported values for solid-state coronene,[34] but correspond to coronene oligomers.[35] Recently published calculations showed that chain oligomers formed by coronene polymerization cannot be distinguished using Raman spectroscopy since their spectra exhibit only rather minor length-dependent differences.[23] The coronene oligomers are insoluble in common solvents[35] and can still be detected in GNR@SWNT samples after a long washing treatment with toluene, while the pristine coronenes are soluble in toluene and can be removed. The position of the nanotube G band shows no change after GNR formation inside, confirming the absence of charge transfer between outer shells of nanotubes and GNRs (Figure 3). This observation is also consistent with the absence of intensity decrease of the E_{11s} band in absorption spectra after filling.

No additional spectral signatures of GNRs in the G mode region have been detected. The response might

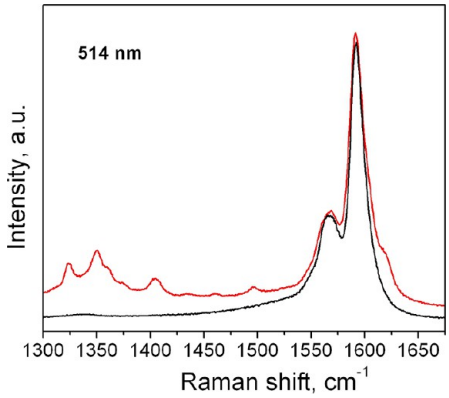

Figure 3. Raman spectra of G and D bands of pristine SWCNTs (in black) and GNR@SWCNTs (in red).

be hindered by the strong resonance components corresponding to the outer SWCNTs. This hypothesis is indirectly confirmed by the investigation of the 2D line. After formation of encapsulated GNRs the width and the shape of the 2D line changes. New components with positions close to the values known for graphene appear in the spectra within the broad 2D peak from the outer SWCNTs (Supporting Information).

The Raman spectra in the RBM (radial breathing mode) spectral range are presented in Figure 4. Filling of SWCNTs with molecules and compounds results in changes of their vibration frequencies.[36,37] We have detected the significant up-shifts in the peak positions for the filled samples (up to 9 cm^{-1}), which are higher compared to the Raman shifts of the stacked coronene columns inside SWCNTs.[33] The nanotubes with similar diameters, demonstrating RBM peak positions around 190 cm^{-1}, can have different up-shifts (from 3 to 9 cm^{-1}) as measured for the two filled samples with different nanotube geometry distributions (Figure 4). The shifts of the RBM mode frequencies together with the broadening of the line widths depend not only on the diameters of host tubes but also on their geometry together with the geometry variations of encapsulated GNRs and their helical twists. Noteworthy to mention is that spectra from GNR@SWCNTs demonstrate no signs

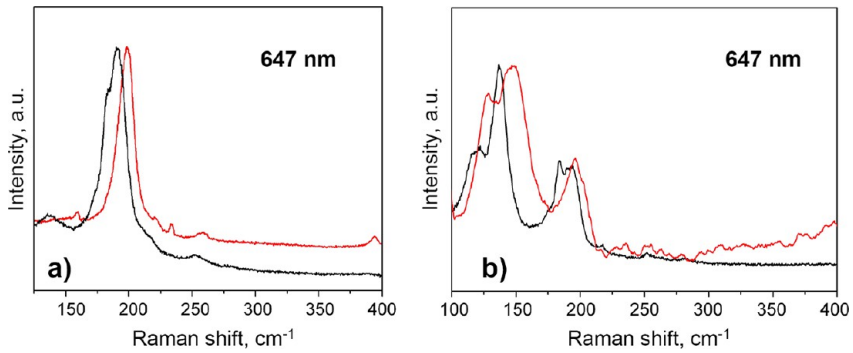

Figure 4. Raman spectra of the RBM band of pristine SWCNTs (in black) and GNR@SWCNTs (in red). (a) SWCNTs with an average diameter of 1.3 nm. (b) SWCNTs with an average diameter of 1.9 nm.

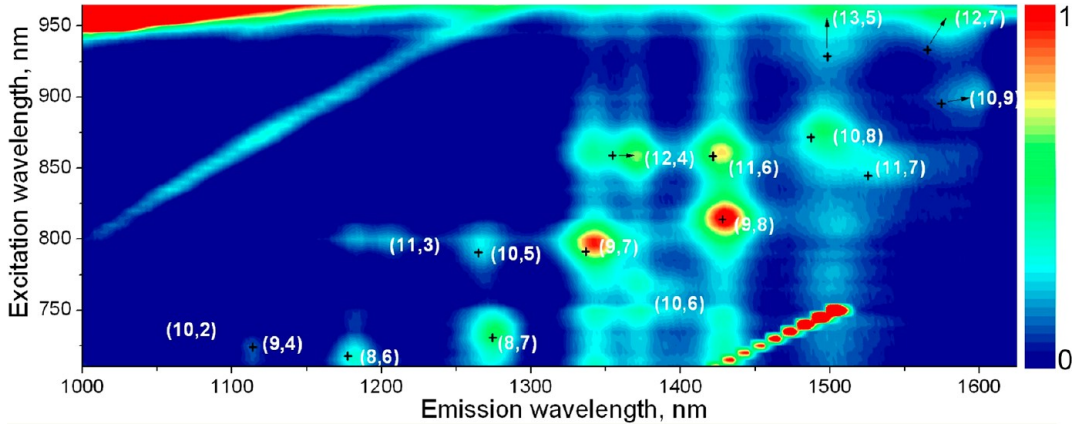

Figure 5. IR PLE contour plot of the GNRs@SWCNTs. Central positions of the peaks from pristine SWCNTs are marked with crosses.

of double-walled carbon nanotubes (DWCNTs). DWCNT formation in nanotubes with diameters similar to those used in our experiments (1.3 nm) requires ultrahigh curvature of inner tubes, and the possible geometries have been studied in detail in the paper by Plank *et al.*[38,39] Considering the relatively large diameter of the coronene molecule (~0.8 nm) and its planar shape, it is rather unlikely that inner nanotubes could form at the very low temperatures used in our experiments (420 °C). Formation of DWCNTs from smaller organic molecules is typically observed at much higher temperatures (~900−1000 °C). However, for perylene (PAH molecule with smaller size compared to coronene) encapsulated in SWCNTs formation of inner nanotubes was not observed even at 1050 °C.[40] On the other hand, theoretical studies showed that graphene nanoribbons can be twisted into nanotubes,[41] which could happen also with dehydrogenated GNRs at very high temperatures. The formation of inner tubes from the GNRs prepared using a coronene precursor was observed recently, but only at much higher temperatures (1250 °C), which is not surprising, as the C−H bonds in hydrogen-terminated nanoribbons are expected to break above ~700 °C.[42]

The IR PLE contour maps of the pristine nanotubes and GNR@SWCNTs are presented in Figure 5. For these measurements carbon nanotubes with an average diameter of 1.3 nm have been suspended in D_2O with DOC salt. After formation of GNRs we still detect the intense response from SWCNTs. However, there are differences in contour maps recorded before and after the synthesis; for example, many PL peaks of SWCNTs in GNR@SWCNT samples demonstrate red shifts. The E_{11} PL peak shifts for SWCNTs with indices (10,9) and (12,7) are up to 11 meV. Taking into account that both initial tubes and GNR@SWCNTs are in the same environment and went through equal sonication treatment, the major reason for the red shift of the PL should be the induced radial strain of the host tubes. In the work of Okazaki *et al.*,[43] where the authors study the changes of PL response after fullerene encapsulation, the red shifts are assigned to strains of SWCNTs together with hybridization of the energy levels between encapsulated molecules and outer tubes. In our case, the measurements have been performed on the nanotubes with diameters near the limit of encapsulation; therefore the radial strain becomes the main mechanism for the band gap modification. Surprisingly, the shifts are detected for nanotubes with diameters smaller than the DFT-estimated limit values for the exothermic encapsulation of stacked coronene columns inside carbon nanotubes.[33] For instance, large

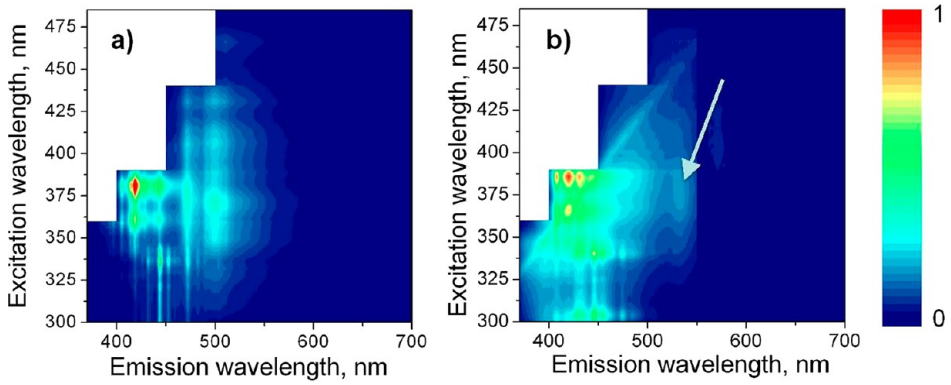

Figure 6. PLE contour plots in the visible spectral range. (a) Coronene molecules in a hexane solution. (b) GNRs@SWCNTs suspended in D_2O. New peak assigned to a GNR is marked with a white arrow. Average diameter of SWCNTs is 1.3 nm.

red shifts in emission have been detected for (12,4) tubes with a diameter of 1.15 nm.

The reason for such peak shifts of narrow diameter tubes might be formation of imperfect and even deformed GNRs inside. PLE measurements indicate that the limit of the nanotube diameter for encapsulation of coronene molecules is around 1.1 nm. It should be noted that structures that are formed inside are determined by the geometry of the host tubes. Besides, such structures appear to be not ideally flat GNRs. Therefore, it is complicated to model the dependence between the outer tube diameters and the induced shifts.

PLE contour maps recorded in the visible spectral range from the same GNR@SWCNT sample and from the reference sample of coronene are presented in Figure 6. Coronene has emission peaks in the visible spectral range up to 550 nm,[44] which correspond to S_1 fluorescence from the singlet and triplet states. Similar peaks are presented on the contour map of the GNR@SWCNT sample. Despite the slight red shifts in excitation of the peaks and their intensity redistribution, the main coronene PL bands are detected in the emission range from 380 to 460 nm in the GNR@SWCNT sample. We could follow the intensity decrease of these peaks performing the washing procedure of the sample with toluene. However, we were not able to remove completely the synthesis side products. Importantly, some PL bands demonstrate no intensity change after the toluene treatment, and, moreover, they are not presented in PLE contour maps of coronene. The additional peak appeared after the synthesis procedure. It is positioned at around 533 nm emission and 377 nm excitation wavelengths (Figure 6b). The peak is resonant and the line width in emission is around 70 meV. We assign this peak to the GNRs formed inside SWCNTs. Taking into account the van der Waals interaction between the inner structure and outer nanotube, the most favorable width of the nanoribbon for a 1.3 nm diameter tube is 0.64 nm. DFT calculations of the dependence between the energy band gap and the width of hydrogen-terminated GNRs

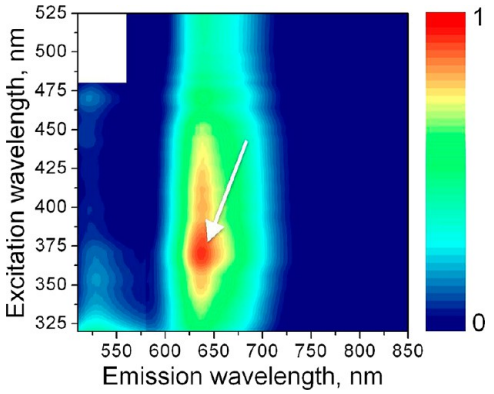

Figure 7. PLE contour plot in the visible spectral range of GNRs@SWCNTs. Maximum of the GNR peak is marked with a white arrow. Average diameter of SWCNTs is 1.9 nm.

performed by Barone *et al.*[21] predicted the oscillation type variation of the band gap as a function of the GNR's width. The value of the PL peak position obtained in our experiment is well within the theoretically predicted ranges of energy band gap for the nanoribbons with a width of around 0.64 nm. As mentioned before, the host tube governs the structure of the inner GNR and therefore its width. To follow the width change of GNRs in PL, we have looked at the GNRs formed in the bigger diameter tubes (Figure 7). For SWCNTs with an average diameter of 1.9 nm we have detected a new peak centered at 639 nm emission and 369 nm excitation wavelengths. This peak is significantly shifted toward the longer wavelengths in emission compared to the peaks detected from the 1.3 nm diameter tube sample. This observation is in agreement with the assumption that GNRs formed in the bigger diameter tubes are wider and have a narrower band gap. According to the previously mentioned DFT calculations, this peak might correspond to the GNR with a width of around 0.93 nm, which is in good agreement with the obtained HRTEM data.[19] Therefore, new PL features that appeared after the synthesis procedure can be reasonably considered as a contribution from GNRs formed inside SWCNTs. Hydrogen-terminated GNRs with a two hexagon width can be

suggested to form inside the smaller diameter nanotubes, while the three hexagon wide GNRs are likely to form inside the 1.9 nm SWCNTs.

In comparison to the coronene stacked columns the PL response from GNRs is markedly different. For coronene columns the main reported PL lines are positioned below 550 nm and demonstrated no dependence on the excitation wavelength in the range between 320 and 366 nm.[33] In our case we have resonance peaks in PLE contour plots with positions located further in the red part of the spectrum and dependent on the width of the GNRs. Therefore, the PLE mapping allows distinguishing various nanostructures formed inside SWCNTs.

The excited-state energies of the encapsulating SWCNTs are below the energies of encapsulated GNRs; however, we are able to obtain a bright PL from the ribbons. Similar phenomena have been reported by Loi *et al.*,[45,46] where authors encapsulated α-sexithiophene (6T) inside SWCNTs, and Okazaki *et al.*[33] for encapsulated coronene molecules. In comparison to the coronene stacked columns the PL response from the GNRs is markedly different. For coronene columns the main reported PL lines are positioned below 550 nm and had no dependence on the excitation in the range between 320 and 366 nm. In our case we have resonance peaks in PLE contour plots with positions located further in the red part of the spectrum and dependent on the width of the GNRs. Therefore, the PLE mapping allows distinguishing various nanostructures formed inside SWCNTs.

Due to a weak energy transfer between GNRs and outer SWCNTs, the PL response of GNR@SWCNTs can be observed simultaneously in IR and visible spectral ranges. This opens up new possibilities to use this material in photonics. A bright PL from encapsulated GNRs can be successfully applied in biology for imaging and sensors. It is important to emphasize that the electronic structure of the encapsulated structures can be controlled by tuning the size of the host tubes. Using SWCNTs of various diameters allows tailoring the properties of the encapsulated material. It is also likely that selection of different "nanographene" precursor molecules and variations of synthesis parameters (*e.g.*, temperature and pressure) will result in formation of GNRs with different geometry and edge types. Confinement of GNRs inside the SWCNTs provides conditions for unusual stability of very narrow GNRs even when they are exposed to the ambient air conditions. Some degradation of GNRs was observed only after several months of air storage. Therefore, GNR@SWCNTs can be proposed as a feasible material for creation of robust nanosized light emitters working at visible wavelengths.

CONCLUSIONS

In conclusion, we studied the optical properties of composite materials prepared using coronene encapsulation and polymerization inside SWCNTs. We demonstrate that GNRs@SWCNTs can be characterized by PLE mapping and distinguished from single molecules encapsulated in SWCNTs. In addition to the strain-induced red shifts of the bands from SWCNTs in the IR spectral range we detected new features corresponding to GNRs in the visible spectral range. PLE mapping allows identifying GNRs with different geometries. For the narrowest detected GNRs the emission wavelength is 533 nm. The PL peak positions of GNRs are in agreement with theoretical studies and HRTEM observations. The simultaneous bright PL response of GNR@SWCNTs in both the IR and visible regions can be used in various photonics applications, *e.g.*, for robust nanosized light emitters.

EXPERIMENTAL SECTION

Sample Preparation. SWCNTs used in the work have been synthesized by the aerosol method[29] and initially were in the form of films. GNRs were synthesized using a confined polymerization and fusion of polycyclic aromatic hydrocarbon (coronene) molecules by annealing of SWCNTs in coronene vapor in an argon or hydrogen atmosphere. The annealing temperature was set at 420 °C in order to reduce the amount of side products, which easily form on the outer walls of the nanotubes. More details on the synthesis process can be found elsewhere.[19] The sample was washed in toluene to remove coronenes from the outside of the SWCNTs. The pristine nanotubes and a novel nanomaterial were examined in the form of both films and suspensions. The suspensions were prepared using a natural bile salt detergent—sodium salt of deoxycholic acid (DOC) in D_2O—in order to individualize SWCNTs. DOC has been shown to be very efficient in solubilizing the individual carbon nanotubes compared with the other commonly used detergents.[47] GNR@SWCNTs (or just SWCNTs) were ultrasonicated in D_2O-dissolved DOC (1 w/v percent) during 15 min. During the sonication process the tube containing the suspension was immersed into cold water. The obtained suspension was centrifuged in a Beckman Coulter Ultra-Max-E centrifuge (MLA-80 rotor) for 0.5 h with an acceleration of 140000*g*. The supernatant was used for the measurements. The coronene powder was dissolved in *n*-hexane for the reference measurements.

Optical Measurements. The PL measurements of GNR@SWCNTs have been performed either directly from the films on the quartz substrates or from the aqueous suspensions. The photoluminescence spectra were recorded with a Horiba Jobin-Yvon NanoLog system supplied with an InGaAs CCD detector (850−1550 nm) and with a photomultiplier (R928P) working in a spectral range of 180−850 nm. Photoluminescence excitation in the UV−vis spectral range was performed with a Xe lamp (250−900 nm).

The optical absorption spectra were recorded using a UV−vis−NIR double-lined spectrophotometer (Perkin-Elmer Lambda 900). The spectral resolution was 0.5 nm in the 200−3000 nm (6.2−0.41 eV) spectral range.

The Raman spectra were recorded using a Jobin Yvon S3000 triple monochromator spectrometer in a microconfiguration. The spectral resolution was 1 cm^{-1}. An Ar−Kr ion laser (Stabilite 2018, Newport) at various wavelengths (from 488 nm (2.54 eV) up to 647 nm (1.92 eV)) was used for excitation in Raman measurements.

Conflict of Interest: The authors declare no competing financial interest.

Acknowledgment. The work was supported by RFBR grant nos. 13-02-01354, 13-02-90719, and 12-02-31581, RAS research projects, Ministry of Education and Science of Russian Federation grant nos. 14.513.12.003 and SP-7362.2013.3, and Academy of Finland. A.T. acknowledges the Swedish Research Council, grant no. 621-2012-3654, and Ångpanneföreningens Forskningsstiftelse.

Supporting Information Available: Details on the photoluminescence excitation mapping. Raman measurements of the 2D line of GNR@SWCNTs. Photoluminescence response from the synthesis side products. This material is available free of charge *via* the Internet at http://pubs.acs.org.

REFERENCES AND NOTES

1. Reich, S., Thomsen, C., Maultzsch, J., Eds. *Carbon Nanotubes*; Wiley: Weinheim, 2004.
2. Bachilo, S. M.; Strano, M. S.; Kittrell, C.; Hauge, R. H.; Smalley, R. E.; Weisman, R. B. Structure-Assigned Optical Spectra of Single-Walled Carbon Nanotubes. *Science* **2002**, *298*, 2361–2366.
3. O'Connell, M. J.; Bachilo, S. M.; Huffman, C. B.; Moore, V. C.; Strano, M. S.; Haroz, E. H.; Rialon, K. L.; Boul, P. J.; Noon, W. H.; Kittrell, C.; *et al*. Band Gap Fluorescence from Individual Single-Walled Carbon Nanotubes. *Science* **2002**, *297*, 593–596.
4. He, M.; Chernov, A. I.; Fedotov, P. V.; Obraztsova, E. D.; Sainio, J.; Rikkinen, E.; Jiang, H.; Zhu, Z.; Tian, Y.; Kauppinen, E. I.; *et al*. Predominant (6,5) Single-Walled Carbon Nanotube Growth on a Copper-Promoted Iron Catalyst. *J. Am. Chem. Soc.* **2010**, *40*, 13994–13996.
5. Hong, G.; Lee, J. C.; Robinson, J. T.; Raaz, U.; Xie, L.; Huang, N. F.; Cooke, J. P.; Dai, H. Multifunctional *in Vivo* Vascular Imaging Using Near-Infrared II Fluorescence. *Nat. Med.* **2012**, *18*, 1841–1846.
6. Travers, J. C.; Morgenweg, J.; Obraztsova, E. D.; Chernov, A. I.; Kelleher, E. J. R.; Popov, S. V. Using the E-22 Transition of Carbon Nanotubes for Fiber Laser Mode-Locking. *Laser Phys. Lett.* **2011**, *8*, 144–149.
7. Tyler, T. P.; Brock, R. E.; Karmel, H. J.; Marks, T. J.; Hersam, M. C. Electronically Monodisperse Single-Walled Carbon Nanotube Thin Films as Transparent Conducting Anodes in Organic Photovoltaic Devices. *Adv. Energy Mater.* **2011**, *1*, 758–791.
8. Avouris, P.; Freitag, M.; Perebeinos, V. Carbon-Nanotube Photonics and Optoelectronics. *Nat. Photonics* **2008**, *2*, 341–350.
9. Lefebvre, J.; Austing, D. G.; Bond, J.; Finnie, P. Photoluminescence Imaging of Suspended Single-Walled Carbon Nanotubes. *Nano Lett.* **2006**, *6*, 1603–1608.
10. Lee, A. J.; Wang, X. Y.; Carlson, L. J.; Smyder, J. A.; Loesch, B.; Tu, X. M.; Zheng, M.; Krauss, T. D. Bright Fluorescence from Individual Single-Walled Carbon Nanotubes. *Nano Lett.* **2011**, *11*, 1636–1640.
11. Chernov, A. I.; Obraztsova, E. D. Photoluminescence of Single-Wall Carbon Nanotube Films. *Phys. Status Solidi B* **2010**, *247*, 2805–2809.
12. Liu, X.; Kuzmany, H.; Ayala, P.; Calvaresi, M.; Zerbetto, F.; Pichler, T. Selective Enhancement of Photoluminescence in Filled Single-Walled Carbon Nanotubes. *Adv. Funct. Mater.* **2012**, *22*, 3202–3208.
13. Nakada, K.; Fujita, M.; Dresselhaus, G.; Dresselhaus, M. S. Edge State in Graphene Ribbons: Nanometer Size Effect and Edge Shape Dependence. *Phys. Rev. B* **1996**, *54*, 17954–17961.
14. Son, Y.-W.; Cohen, M. L.; Louie, S. G. Energy Gaps in Graphene Nanoribbons. *Phys. Rev. Lett.* **2006**, *98*, 216803–206807.
15. Han, M. Y.; Oezyilmaz, B.; Zhang, Y.; Kim, P. Energy Band-Gap Engineering of Graphene Nanoribbons. *Phys. Rev. Lett.* **2007**, *98*, 206805–206809.
16. Datta, S. S.; Strachan, D. R.; Khamis, S. M.; Johnson, A. T. C. Crystallographic Etching of Few-Layer Graphene. *Nano Lett.* **2008**, *8*, 1912–1915.
17. Kosynkin, D. V.; Higginbotham, A. L.; Sinitskii, A.; Lomeda, J. R.; Dimiev, A.; Price, B. K.; Tour, J. M. Longitudinal Unzipping of Carbon Nanotubes to Form Graphene Nanoribbons. *Nature* **2009**, *458*, 872–876.
18. Cai, J.; Ruffieux, P.; Jaafar, R.; Bieri, M.; Braun, T.; Blankenburg, S.; Muoth, M.; Seitsonen, A. P.; Saleh, M.; Feng, X.; *et al*. Atomically Precise Bottom-Up Fabrication of Graphene Nanoribbons. *Nature* **2010**, *466*, 470–473.
19. Talyzin, A. V.; Anoshkin, I. V.; Krasheninnikov, A. V.; Nieminen, R. M.; Nasibulin, A. G.; Jiang, H.; Kauppinen, E. I. Synthesis of Graphene Nanoribbons Encapsulated in Single-Walled Carbon Nanotubes. *Nano Lett.* **2011**, *11*, 4352–4356.
20. Chuvilin, A.; Bichoutskaia, E.; Gimenez-Lopez, M. C.; Chamberlain, T. W.; Rance, G. A.; Kuganathan, N.; Biskupek, J.; Kaiser, U.; Khlobystov, A. N. Self-Assembly of a Sulphur-Terminated Graphene Nanoribbon within a Single-Walled Carbon Nanotube. *Nat. Mater.* **2011**, *10*, 687–692.
21. Barone, V.; Hod, O.; Scuseria, G. E. Electronic Structure and Stability of Semiconducting Graphene Nanoribbons. *Nano Lett.* **2006**, *6*, 2748–2754.
22. Lebedeva, I. V.; Popov, A. M.; Knizhnik, A. A.; Khlobystov, A. N.; Potapkin, B. V. Chiral Graphene Nanoribbon Inside a Carbon Nanotube: Ab Initio Study. *Nanoscale* **2012**, *4*, 4522–4529.
23. Fujihara, M.; Miyata, Y.; Kitaura, R.; Nishimura, Y.; Camacho, C.; Irle, S.; Iizumi, Y.; Okazaki, T.; Shinohara, H. Dimerization-Initiated Preferential Formation of Coronene-Based Graphene Nanoribbons in Carbon Nanotubes. *J. Phys. Chem. C* **2012**, *116*, 15141–15145.
24. Li, Y.; Sun, F.; Li, H. Helical Wrapping and Insertion of Graphene Nanoribbon to Single-Walled Carbon Nanotube. *J. Phys. Chem.* **2011**, *115*, 18459–18467.
25. Akatyeva, E.; Dumitrica, T. Chiral Graphene Nanoribbons: Objective Molecular Dynamics Simulations and Phase-Transition Modeling. *J. Chem. Phys.* **2012**, *137*, 234702–234710.
26. Khlobystov, A. N. Carbon Nanotubes: From Nano Test Tube to Nano-Reactor. *ACS Nano* **2011**, *5*, 9306–9312.
27. Chamberlain, T. W.; Biskupek, J.; Rance, G. A.; Chuvilin, A.; Alexander, T. J.; Bichoutskaia, E.; Kaiser, U.; Khlobystov, A. N. Size, Structure, and Helical Twist of Graphene Nanoribbons Controlled by Confinement in Carbon Nanotubes. *ACS Nano* **2012**, *6*, 3943–3953.
28. Zhang, D.-B.; Dumitrica, T. Effective-Tensional-Strain-Driven Bandgap Modulations in Helical Graphene Nanoribbons. *Small* **2011**, *7*, 1023–1027.
29. Tian, Y.; Timmermans, M.; Kivistö, S.; Nasibulin, A. G.; Zhu, Z.; Jiang, H.; Okhotnikov, O. G.; Kauppinen, E. I. Tailoring the Diameter of Single-Walled Carbon Nanotubes for Optical Applications. *Nano Res.* **2011**, *4*, 807–815.
30. Weisman, R. B.; Bachilo, S. M. Dependence of Optical Transition Energies on Structure for Single-Walled Carbon Nanotubes in Aqueous Suspension: An Empirical Kataura Plot. *Nano Lett.* **2003**, *9*, 1235–1238.
31. Fedotov, P. V.; Chernov, A. I.; Talyzin, A. V.; Suarez, I. L.; Anoshkin, I. V.; Nasibulin, A. G.; Kauppinen, E. I.; Obraztsova, E. D. Optical Study of Nanotube and Coronene Composites. *J. Nanoelectron. Optoelectron.* **2013**, *8*, 16–22.
32. Yang, L.; Han, J. Electronic Structure of Deformed Carbon Nanotubes. *Phys. Rev. Lett.* **2000**, *85*, 154–157.
33. Okazaki, T.; Iizumi, Y.; Okubo, S.; Kataura, H.; Liu, Z.; Suenaga, K.; Tahara, Y.; Yudasaka, M.; Okada, S.; Iijima, S. Coaxially Stacked Coronene Columns inside Single-Walled Carbon Nanotubes. *Angew. Chem., Int. Ed.* **2011**, *50*, 4853–4857.
34. Fleischer, U.; Pulay, P. Raman Spectrum of Coronene: A Scaled Quantum Mechanical Force Field Study. *J. Raman Spectrosc.* **1998**, *29*, 473–481.
35. Talyzin, A. V.; Luzan, S. M.; Leifer, L.; Akhtar, S.; Fetzer, J.; Cataldo, F.; Tsybin, Y. O.; Tai, C. V.; Dzwilewski, A.; Moons, E. Coronene Fusion by Heat Treatment: Road to Nanographenes. *J. Phys. Chem. C* **2011**, *115*, 13207–13214.
36. Cambré, S.; Schoeters, B.; Luyckx, S.; Goovaerts, E.; Wenseleers, W. Experimental Observation of Single-File

Water Filling of Thin Single-Wall Carbon Nanotubes Down to Chiral Index (5,3). *Phys. Rev. Lett.* **2010**, *104*, 207401.
37. Kawai, M.; Kyakuno, H.; Suzuki, T.; Igarashi, T.; Suzuki, H.; Okazaki, T.; Kataura, H.; Maniwa, Y.; Yanagi, K. Single Chirality Extraction of Single-Wall Carbon Nanotubes for the Encapsulation of Organic Molecules. *J. Am. Chem. Soc.* **2012**, *134*, 9545–9548.
38. Plank, W.; Pfeiffer, R.; Schaman, C.; Kuzmany, H.; Calvaresi, M.; Zerbetto, F.; Meyer, J. Electronic Structure of Carbon Nanotubes with Ultrahigh Curvature. *ACS Nano* **2010**, *4*, 4515–4522.
39. Pfeiffer, R.; Kuzmany, H.; Simon, F.; Bokova, S. N.; Obraztsova, E. Resonance Raman Scattering from Phonon Overtones in Double-Wall Carbon Nanotubes. *Phys. Rev. B* **2005**, *71*, 155409–155416.
40. Fujita, Y.; Bandow, S.; Iijima, S. Formation of Small-Diameter Carbon Nanotubes from PTCDA Arranged inside the Single-Wall Carbon Nanotubes. *Chem. Phys. Lett.* **2005**, *413*, 410–414.
41. Kit, O. O.; Tallinen, T.; Mahadevan, L.; Timonen, J.; Koskinen, P. Twisting Graphene Nanoribbons into Carbon Nanotubes. *Phys. Rev. B* **2012**, *85*, 085428–085437.
42. Botka, B.; Füstös, M. E.; Klupp, G.; Kocsis, D.; Székely, E.; Utczás, M.; Simándi, B.; Botos, Á.; Hackl, R.; Kamarás, K. Low-Temperature Encapsulation of Coronene in Carbon Nanotubes. *Phys. Status Solidi B* **2012**, *249*, 2432–2435.
43. Okazaki, T.; Okubo, S.; Nakanishi, T.; Joung, S.; Saito, T.; Otani, M.; Okada, S.; Bandow, S.; Iijima, S. Optical Band Gap Modification of Single-Walled Carbon Nanotubes by Encapsulated Fullerenes. *J. Am. Chem. Soc.* **2008**, *130*, 4122–4128.
44. Nijegorodov, N.; Mabbs, R.; Downey, W. S. Evolution of Absorption, Fluorescence, Laser and Chemical Properties in the Series of Compounds Perylene, Benzo(ghi)perylene and Coronene. *Spectrochim. Acta, Part A* **2001**, *57*, 2673–2685.
45. Loi, M. A.; Gao, J.; Cordella, F.; Blondeau, P.; Menna, E.; Bártová, B.; Hébert, C.; Lazar, S.; Botton, G. A.; Milko, M.; *et al.* Encapsulation of Conjugated Oligomers in Single-Walled Carbon Nanotubes: Towards Nanohybrids for Photonic Devices. *Adv. Mater.* **2010**, *22*, 1635–1639.
46. Yanagi, K.; Kataura, H. Carbon Nanotubes: Breaking Kasha's Rule. *Nat. Photonics* **2010**, *4*, 200–201.
47. Wenseleers, W.; Vlasov, I.; Goovaerts, E.; Obraztsova, E. D.; Lobach, A. S.; Bouwen, A. Efficient Isolation and Solubilization of Pristine Single-Walled Nanotubes in Bile Salt Micelles. *Adv. Funct. Mater.* **2004**, *14*, 1105–1112.